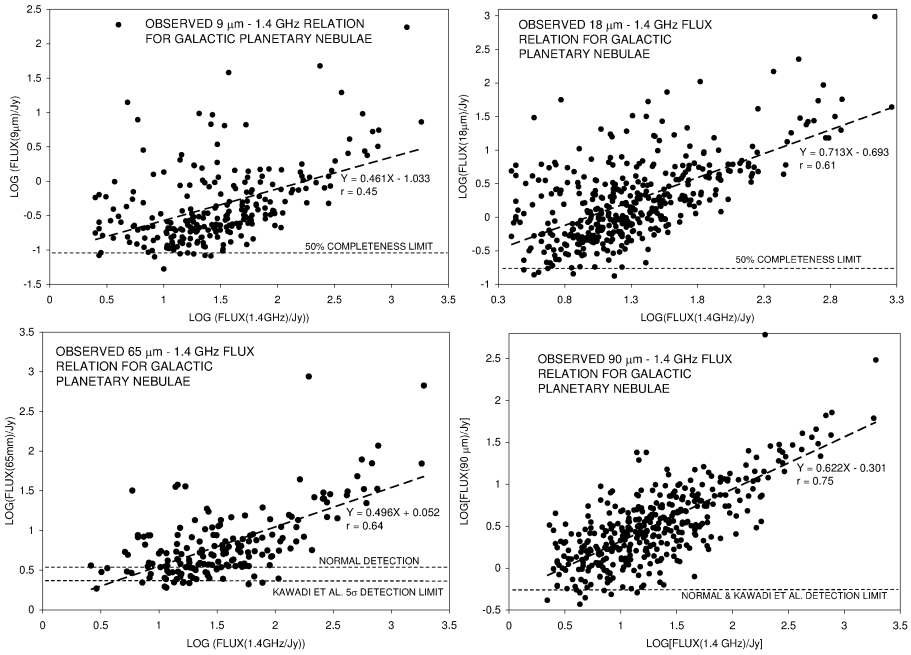

Fig. 12. The variation of infrared fluxes with respect to 1.4 GHz emission, where we illustrate the trends for four of the AKARI photometric channels. All of the results indicate linear trends. Note how the limiting AKARI and radio sensitivities restrict the numbers of observed sources, and appreciably modify the trends. Least-squares fits to the data are indicated using dashed lines, for which we indicate equations and correlation coefficients (r) within each of the panels.

by the upper line). It is therefore clear that whilst certain 5 GHz fluxes derive from partially or fully opaque regimes, the vast majority of 1.4 GHz results are optically thin - and yield fluxes proportional to the total masses of ionised gas.

Phillips (2007) has noted that higher 5 GHz/ 1.4 GHz ratios are confined to more compact sources, where density and emission measures are larger. This is also noted for the PNe investigated here (Figure 11, lower panel), where it is clear that higher 5 GHz opacities arise when diameters are < 0.07 pc; a range similar to that determined for higher values of $T_{\rm GR}$ (§ 3.2).

The variation of infrared emission with 1.4 GHz flux is illustrated in Figure 12, where it is clear that there is a linear relation between the two sets of data. Such trends are strongly affected by a variety of biases, however, and these greatly modify the perceived gradients. In the first place, distance-squared spreading of the fluxes would tend to lead to a one-to-one relation. It is also apparent that source numbers are truncated where $F_\nu(1.4\ {\rm GHz}) \leq 3$ Jy, corresponding to the sensitivity limit of the Condon et al. (1998) survey.

Even greater biases arise from the limiting sensitivities of the differing AKARI channels, however, and we have indicated these using horizontal dashed lines. We have included values corresponding to 50% source detection rates; a so-called "normal mode" detection limit quoted in the FIS Bright Source Catalogue (Yamamura et al. 2010); and the 5σ detection limit quoted by Kawada et al. (2007). Most of these limits are mutually consistent, and accord with the fall-offs in the numbers of PNe. The result, for the 9 and 65 μm results, is for an apparent flattening of the trends. It is apparent however that the 90 and 18 μm samples are significantly more complete, and trends are close to those expected for unbiased samples of PNe. We shall therefore be using these trends to assess variations in q_{18} and q_{90}.

We should finally add that detection limits at 140 and 160 μm are even higher, whilst PNe fluxes tend to be lower. This leads to extraordinarily strong truncations in the numbers of PNe, and we have excluded these results from the present analysis.

Distance corrected measures of the fluxes are illustrated in Figure 13. We note that the linear trends in Figure 12 have now largely disappeared, although the scatter between the nebulae is as large